Ezequiel V. Albano

Articles you may be interested in

Dynamic response of an irreversible catalytic reaction to periodic variation of the reactant's pressure
J. Chem. Phys. **112**, 3890 (2000); 10.1063/1.480931

Erratum: "Surface roughening: Kinetics, adsorbate-induced effects, and manifestation in catalytic reactions" [J. Chem. Phys. 108, 4582 (1998)]
J. Chem. Phys. **109**, 7649 (1998); 10.1063/1.477387

Monte Carlo simulations of a surface reaction model showing spatio-temporal pattern formations and oscillations
J. Chem. Phys. **108**, 5921 (1998); 10.1063/1.476003

Surface roughening: Kinetics, adsorbate-induced effects, and manifestation in catalytic reactions
J. Chem. Phys. **108**, 4582 (1998); 10.1063/1.476504

Dynamic behavior of the monomer–monomer surface reaction model with adsorbate interactions
J. Chem. Phys. **107**, 7397 (1997); 10.1063/1.474977

On the influence of reactant's induced surface transformations in the behavior of a heterogeneously catalyzed dimer–monomer reaction model

Ezequiel V. Albano[a]

Instituto de Investigaciones Fisicoquímicas Teóricas y Aplicadas, (INIFTA), Facultad de Ciencias Exactas, Universidad Nacional de La Plata, Sucursal 4, Casilla de Correo 16, (1900) La Plata, Argentina

A surface reaction model for the catalyzed reaction $A + (\frac{1}{2})B_2 \rightarrow AB$ is studied by means of Monte Carlo simulations. Motivated by experiments on the catalytic oxidation of CO on certain Pt surfaces; i.e., $A \equiv CO$, $B_2 \equiv O_2$, and $AB \equiv CO_2$; it is assumed that the catalyst surface undergoes reactant's induced reversible phase transitions (RIRPT's) between two different structures, i.e., a stable (reconstructed) phase in the low (high) A-coverage regime. Also the sticking coefficient of B_2-species depends on the surface structure, being negligible in the stable phase. Two cases are studied in detail depending on whether the RIRPT's involve the whole surface and are due to the average coverage of the sample or, on the other hand, they are restricted to small patches of the surface and are driven by the local coverage. For the case of global RIRPT's, the reactive regime of the system exhibits self-sustained oscillatory behavior. However, considering local RIRPT's oscillations are observed in finite samples but it is shown that they will vanish in the thermodynamic limit. © *1998 American Institute of Physics.* [S0021-9606(98)50340-6]

I. INTRODUCTION

The understanding of the behavior of surface reaction systems is a permanent goal in the fields of theoretical and applied research. From the theoretical point of view, the study of heterogeneously catalyzed reactions is very attractive because such systems often exhibit a rich and complex nonlinear dynamic behavior which may include multistability, oscillations, chemical waves, poisoning, bifurcations, chaos, phase transitions, etc. Furthermore, from the point of view of useful applications, the development of more effective catalysts is extremely challenging due to the economic impact in the production of numerous chemical substances.

Monte Carlo computer simulation methods are powerful tools for the study of surface reaction processes (for a review see, e.g., Ref. 1). The use of these methods has become very fashionable after the publication of the pioneering work of Ziff, Gulari, and Barshad (ZGB);[2] for reviews see e.g., Refs. 1, 3, and 4. The ZGB-model deals with the monomer–dimer reaction $2A + B_2 \rightarrow 2AB$ which mimics the oxidation of carbon monoxide, i.e., A is CO, B_2 is O_2, and AB is CO_2. The ZGB is a lattice gas reaction model, where it is assumed that the reaction proceeds according to Langmuir–Hinshelwood mechanism

$$A(g) + S \rightarrow A(a), \tag{1}$$

$$B_2(g) + 2S \rightarrow 2B(a), \tag{2}$$

$$A(a) + B(a) \rightarrow AB(g) + 2S, \tag{3}$$
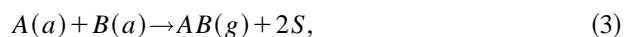
where S is an empty site on the surface, while (a) and (g) refer to the adsorbed and gas phase, respectively.

The relative impingement rates of A- and B_2-species, which are proportional to their partial pressures are normalized ($Y_A + Y_B = 1$), so the ZGB model has a single parameter, i.e., Y_A. For more details on the ZGB model see e.g., Refs. 1 and 2.

Figure 1 shows plots of the rate of AB production (R_{AB}) and the surface coverage with A (θ_A) and B (θ_B) species versus Y_A. So, just at $Y_{1A} \cong 0.3907$ and $Y_{2A} \cong 0.5256$, the ZGB model exhibits irreversible phase transitions (IPT's) between a reactive regime with sustained production of AB-species and poisoned states with B- and A-species, respectively. The smooth IPT at Y_{1A} is of second order and the abrupt IPT at Y_{2A} is of first order. Experimental evidences of a first-order ''transitionlike'' behavior have been reported for the catalytic oxidation of carbon monoxide on $Pt(210)$ and $Pt(111)$.[5,6] Here, we used the term transitionlike because an abrupt decrease of R_{AB} is in fact observed when the pressure is tuned around a critical value, however, the formation of a true poisoned state with CO is prevented by the (rather small) desorption rate of such species. For detailed studies on the first-order IPT within the ZGB framework see e.g., Refs. 7–9 It should be pointed out that with the use of an additional parameter, namely the desorption probability of A-species, it is possible to prevent the occurrence of the first-order IPT in qualitative agreement with the experimental findings.[10,11]

In spite of the fact that second-order transition has not been observed in experiments of oxidation of carbon monoxide in particular as well as in related irreversible processes in general, it has extensively been studied using a variety of theoretical approaches.[12–15] The main finding is that it belongs to the universality class of directed percolation.[16] Obviously, this failure of the ZGB model is due to the crude assumptions involved, for example, diffusion of adsorbed

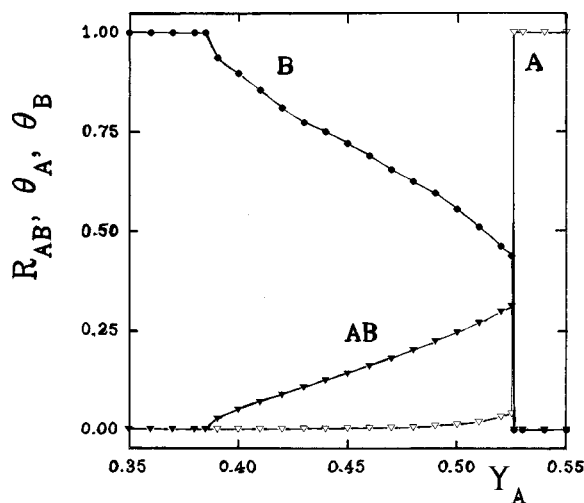[a]Fax: 0054–21–254642; Electronic mail: ealbano@isis.unlp.edu.ar

FIG. 1. Plots of the rate of AB production (R_{AB}) and the surface coverage with A (θ_A) and B (θ_B) species vs Y_A, for the ZGB model.

species is neglected, desorption of the reactants is not considered, lateral interactions are ignored, etc. Efforts to overcome these shortcomings has been performed, see e.g., Refs. 10, 11, 17–19, etc.

So far, the ZGB model and many studied variants of the dimer–monomer reaction process, do not account for a relevant characteristic of certain reaction processes which is very well documented experimentally. Using low electron energy diffraction patterns, measurements of adsorbate induced work function changes, mass spectrometry analysis, and other modern techniques it has been established that the surface of some catalysts undergoes structural reconstructions which are coupled with the reactant's coverages.[20,21] Within this context the aim of this manuscript is to propose and study a modified version of the ZGB model which accounts for the observed structural reconstructions of the surface. Two cases, the first one considering the global reconstruction of the surface, while the second one assuming local reconstructions of surface patches of different size, are studied. It is shown that, in both cases, the surface reconstruction causes the oscillatory behavior of the reactant's coverages as observed in actual experiments,[20,21] however, for local reconstructions, oscillations are restricted to finite samples and they vanish in the thermodynamic limit.

II. DESCRIPTION OF THE MODEL AND THE SIMULATION TECHNIQUE

It is well known that the catalytic oxidation of CO on certain Pt surfaces exhibits oscillatory behavior, within a restricted range of pressures and temperatures. Such oscillations are coupled with adsorbate-induced surface phase transitions.[20,21] In fact, in their clean states the reconstructed surfaces of some crystallographic planes; e.g., $Pt(100)$ and $Pt(110)$ are thermodynamically stable. However, the reconstruction can be lifted by adsorbed species such as CO, NO, O_2, etc. So, the atoms of the topmost layer move back into their 1×1 positions. The adsorbate-induced transition (AIT) between the reconstructed and the 1×1 phases is reversible and, therefore, can be driven by critical adsorbate coverages.

For a detailed discussion on the nature of the transition see Refs. 20 and 21. The observed variations in the catalytic activity occur because due to the change in the surface geometry, which takes place as a consequence of the AIT's, also the adsorption properties of the surface change. On Pt surfaces the O_2 sticking coefficient (S_{O_2}) is highly structure dependent, and since the oscillations occur when oxygen adsorption is rate limiting, the catalytic activity is thus periodically modulated by the AIT's. Oxygen adsorption experiments on $Pt(100)$ show that $S_{O_2} \cong 0.1$ on the 1×1 phase while a drastic decreases of about 2 to 3 orders of magnitude is observed for the reconstructed phase. On $Pt(110)$ a variation of S_{O_2} is also observed but it is smaller. A single oscillatory cycle can be described as follows (see the schema below):[20]

CO coverage	high	low
Surface structure	1×1	reconstructed
O_2 adsorption	S_{O_2} large	S_{O_2} small
Catalytic activity	high	low

Starting with a CO covered 1×1 surface one has a high S_{O_2} value. This leads to a high reaction rate causing the CO-coverage (θ_{CO}) to decrease. Below a certain critical value, θ_{1CO}, the surface relaxes into the reconstructed phase. Now S_{O_2} is small and the reaction rate also decreases causing the growth of θ_{CO}. Above another critical value, θ_{2CO}, an AIT of the surface takes place and the catalyst recovers the initial 1×1-structure again.

In order to simulate the ZGB model with adsorbate induced surface phase transitions we have used a square lattice of side L to represent the catalytic surface. Let us first describe the model which assumes the global reconstruction of the surface. Let θ_{1A} and θ_{2A} be the critical coverages at which the reversible phase transitions of the surface take place, and S_{1B_2} and S_{2B_2} the corresponding sticking probabilities of B_2-species . The Monte Carlo algorithm for the simulation is as follows: (i) A or B_2 molecules are selected randomly with relative probabilities Y_A and $Y_B = 1 - Y_A$, respectively. These probabilities are the relative impingement rates of both species, which are proportional to their partial pressures. Due to the normalization, $Y_A + Y_B = 1$, we used Y_A as a parameter. If the selected species is A, one surface site is selected at random, and if that site is vacant, A is adsorbed on it Eq. (1). Otherwise, if that site is occupied, the trial ends and a new molecule is selected. If the selected species is B_2 a pair of nearest-neighbor sites is selected at random. Only if they are both vacant adsorption proceeds according to Eq. (2) but with probabilities S_{1B_2} or S_{2B_2} depending on the structure of the surface. (ii) After each adsorption event, the nearest-neighbors sites of the added molecule are examined in order to account for the reaction given by Eq. (3). If more than one [B(a),A(a)] pairs are identified, a single one is selected at random and removed from the surface. Notice that the structure of the whole surface is updated after each event comparing θ_A with the critical coverages θ_{1A} and θ_{2A}.

Also, local reconstructions of the surface are considered. Here, the lattice of size $L\times L$ is the result of the addition of

small patches of size $L_p \times L_p$, such as $L = nL_p$, where n is an integer with $n \gg 1$. Each atom of a dimer can adsorb on adjacent patches and also neighboring A- and B-species adsorbed on different patches are allowed to react. In this way correlations may develop through the whole sample via neighboring patches. The reconstruction rules described above are now applied to the individual patches considering the local coverages.

The Monte Carlo time step (t) involves L^2 trials, so each site of the lattice is visited once, on average, during each time unit. Simulations are started with empty lattices. The first 10^4 time steps are disregarded in order to allow the establishment of a stationary state, then subsequent 8×10^4 time steps are used to compute the averaged quantities of interest, i.e., the coverages with A- and B-species given by θ_A and θ_B, and the rate of AB production R_{AB}, respectively. Unless otherwise stated, simulations are performed assuming $S_{1B_2} = 1.0$, $S_{2B_2} = 0.0$, $\theta_{1A} = 0.10$ and $\theta_{2A} = 0.485$. It is found that variations of these parameters cause only qualitative changes in the results. A similar model has earlier been proposed and studied by Moller et $al.$[22] In that work, cellular automata simulations were performed mostly aimed to describe the propagation of two-dimensional patterns. In contrast, in the present work our interest is focused to the study of the irreversible critical behavior of the reaction process in a model which incorporates, to the ZGB's framework, the influence of both local and global adsorbate induced reversible structural transitions of the catalyst surface. Very recently, Vigil et $al.$[23] have reported mean-field and lattice-gas studies of the oscillatory dynamics of a variant of the ZGB model. In contrast to the present work, oscillations are introduced allowing the reversible adsorption of an inert species.

III. RESULTS AND DISCUSSION

A. The phase diagram

Figure 2 shows plots of the time averaged rate of AB-production versus Y_A for the ZGB model with and without reconstructions. For the standard ZGB model a narrow reactive regime within the range $Y_{1A} < Y_A < Y_{2A}$ is observed as discussed above in Fig. 1. For the case of global reconstruction of the surface, the phase diagram retains a discontinuous IPT of first order at the critical point $Y_{Ac} \cong 0.5235 \pm 0.0005$, i.e., a value very close but slightly smaller than that of the standard ZGB model given by $Y_{2A} \cong 0.525\,60 \pm 0.000\,01$.[9]

For the model with global reconstructions it is also very interesting to discuss the output of reaction products for each state of the surface. Figure 3 shows plots of R_{AB} versus Y_A for the surface phases PL and PH of low and high B_2 sticking coefficients, respectively. R_{AB}-values are averaged over the time that the surface remains at the respective state. For the PH the rate of AB-production is almost independent of Y_A in contrast to the PL where such a rate increases monotonously with Y_A till the critical edge. Let τ_{PL} and τ_{PH} be the average periods of time that the surface elapses in the states PL and PH, respectively. So, the number of AB-species produced during each period is given by $N_{AB-X} = R_{AB}\tau_X$, with $X = PL, PH$. Plots of N_{AB-X} versus Y_A are also shown
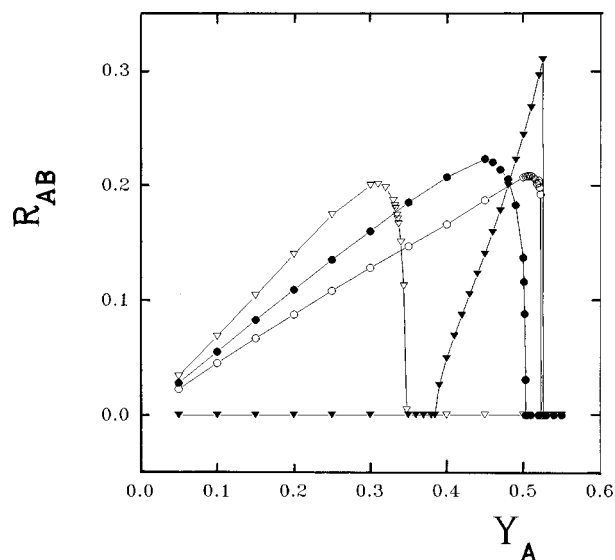

FIG. 2. Plots of the rate of AB production (R_{AB}) vs Y_A for the ZGB model and the same model with adsorbate induced surface phase transitions. (▼) standard ZGB model; (○)ZGB model with global reconstructions; (●) and (▽) ZGB model with local reconstructions $L_p = 8$ and $L_p = 3$, respectively. Most data is taken using $L = 256$ and $L = 258$ but close to criticality $L = 512$ and $L = 516$ are used.

in Fig. 3. It is observed that the output of AB-species during the PH surface state can be several orders of magnitude higher than the output corresponding to the PL phase, particularly close to criticality since $\tau_{PH} \to \infty$ for $Y_A \to Y_{2A}$ due to poisoning with A-species. However, for the LH state R_{AB} increases but τ_{LH} decreases for $Y_A \to Y_{2A}$, so a compensatory effect is observed and the number of AB-species produced remains almost independent of Y_A.
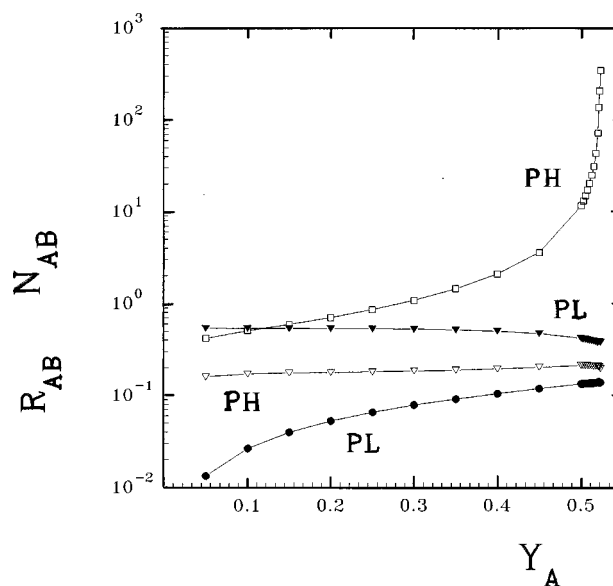

FIG. 3. Plots of the rate of AB-production (R_{AB}) and the number of AB-species desorbed from the surface (N_{AB}) vs Y_A for the ZGB model with global adsorbate induced surface phase transitions. Data is shown for the surface states with low (PL) and high (PH) B_2 sticking coefficient; respectively; as indicated in the figure. For more details see the text.
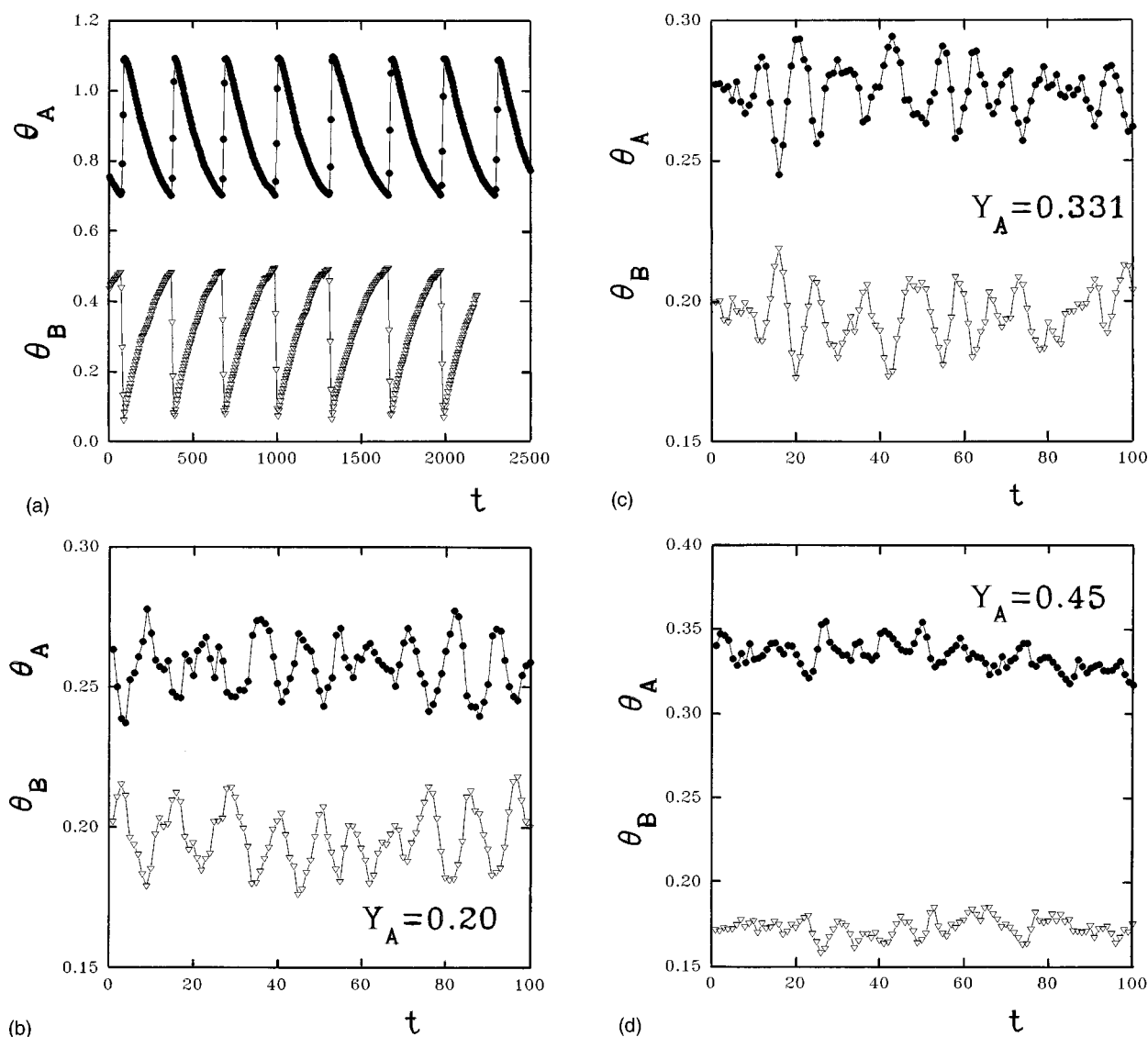
FIG. 4. Plots of θ_A and θ_B vs time obtained using lattice of size $L=512$. The origin of the time axis is set after disregarding 10^4 Monte Carlo time steps in order to achieve the stationary regime. (a) Data taken at $Y_A=0.50$ for the ZGB model with global reconstructions. Note that θ_A-values are shifted up by 0.5 for the sake of clarity. (b), (c), and (d) Plots of θ_A and θ_B vs time for the ZGB model with local reconstructions with $L_p=8$ and measured at different values of Y_A.

Considering local reconstructions of the surface, one also observes the occurrence of IPT's between the reactive regime and the poisoned state with A-species. However, these transitions are less abrupt and become slightly rounded. This effect is due to the cooperative contribution of many individual patches which may not necessarily be in the same surface structural state and consequently their coverages and rates of AB-production may be different. More details on the collective behavior of the patches will be discussed in Sec. III C. It should also be noted that the location of the ITP is quite sensitive to the size of the patches; i.e., one has $Y_{Ac} \cong 0.3485 \pm 0.0005$ and $Y_{Ac} \cong 0.5035 \pm 0.0005$ for $L_p=3$ and $L_p=8$, respectively.

Summing up, the results presented in Fig. 2 for the ZGB model with adsorbate induced structural transitions of the surfaces are in qualitative agreement with experimental the results of Ehsasi et al.[5,6] for the catalytic oxidation of CO on Pt single crystal surfaces. A minor difference is that, in ac-

tual experiments, a truly CO-poisoned state is not achieved due to CO-desorption. This fact can be easily taken into account in the simulations and the result is that for rather small desorption probabilities of A-species one also observes an abrupt decrease in the rate of production which suggest a first-order transition.[10,11]

B. The oscillatory behavior

Figure 4(a) shows the temporal dependence of the reactant's coverages measured at $Y_A=0.50$ for the ZGB model with global surface reconstruction. A self-sustained oscillatory behavior is clearly observed. Increments in the coverage of A-species are in phase with drops in B-coverage, and vice versa. Oscillations exhibit a well defined *periodicity* and for the example shown in Fig. 4(a) the average periods for the phases of low and high B_2 sticking coefficients are $\tau_{PL} \cong 3.11 \pm 0.02$ and $\tau_{PH} \cong 54.8 \pm 0.2$, respectively. Figure 5(a)
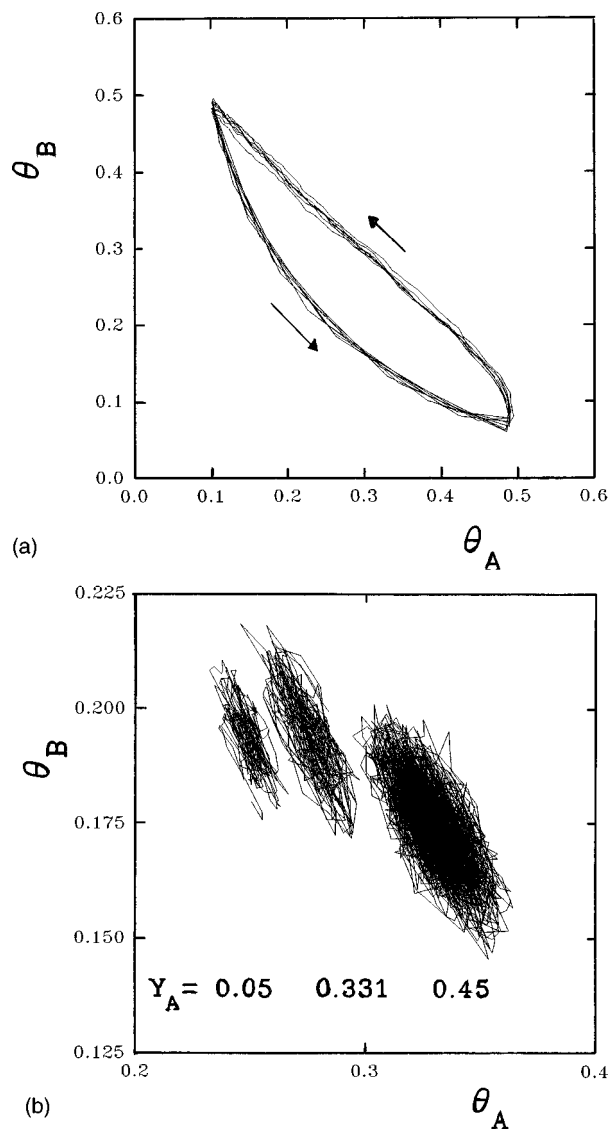
(a)

(b)

FIG. 5. Plots of θ_B vs θ_A obtained from the data shown in Fig. 4 for L = 512. (a) Data taken at Y_A=0.50 for the ZGB model with global reconstructions and showing closed loops which evolve anti-clockwise in time. (b) Data corresponding to the ZGB model with local reconstructions (L_p = 8) and different values of Y_A, as indicated in the figure.

shows that, within the reactive oscillatory regime, a plot of θ_B versus θ_A describes closed loops. Trajectories due to different loops are quite close to each other, indicating that the range of coexisting reactant's coverages during the development of the reaction is very narrow.

When approaching the critical threshold oscillations become *nonperiodic*, that is oscillations of a short period may be followed by long-lived oscillations. It seems that the occurrence of oscillations of different periods does not follow any regular behavior. This observation may suggest stochastic or chaotic behavior, however, a more precise characterization of the process deserves careful study.[24]

Considering local reconstructions of the catalyst surface, the oscillatory behavior still remains in finite samples, as e.g., it is shown in Figs. 4(b)–4(d), for patches of size L_p = 8 and different values of Y_A. Due to the cooperative contribution of different patches having distinct surface structure

and consequently different sticking coefficient of B_2-species, oscillations are quite irregular and the determination of the characteristic periods (or frequencies) may require a Fourier analysis.[24] Observation of Figs. 4(b)–4(d) also reveals that the amplitude of the oscillations depends on Y_A and when approaching the critical point the amplitude decreases in agreement with the fact that very close to criticality the high coverage with A-species prevents the reconstruction of the surface and oscillations are no longer observed.

Figure 5(b) shows plot of θ_B versus θ_A obtained at different values of Y_A for the ZGB model with local reconstructions. In contrast to the narrow and well defined loops characteristic of the ZGB model with global reconstructions [Fig. 5(a)], now one observes dense patterns due to the intersection of the various trajectories. Consequently, one has a wide range of available coexisting reactant's coverages during the development of the reaction.

C. The collective behavior of surface's patches and finite size effects

Let us consider the ZGB model with local reconstructions. Simulations are started far from the stationary state, with all patches having the same surface structure. During the stochastic evolution of the reaction system, different patches may adopt different structures and when arriving to the stationary state, the homogeneous surface structure of the initial configuration may no longer remain. Patches with different structures have different physical properties because the adsorption probability of B_2-species is structure sensitive. Therefore, the reaction proceeds at distinct rates on the various patches causing the rounding of the peaks in plots of R_{AB} versus Y_A (see e.g., Fig. 2) and the occurrence of irregular oscillations [see e.g., Figs. 4(b)–4(d)]. In order to achieve a deeper understanding of the collective behavior of surface's patches a *surface state order parameter S* can be defined according to

$$S = \frac{|N_{LS} - N_{HS}|}{N_{LS} + N_{HS}}, \qquad (4)$$

where N_{LS} and N_{HS} are the number of patches with surface structures corresponding to the low and high B_2 sticking coefficients, respectively. According to this definition one has $S=1$ when all patches are in the same surface state but S =0 if the surface has the same number of patches of each type. Simulations are carried out with $L_p=8$ and finite size effects are studied using lattices of sizes between $L=32$ and $L=512$. For the largest lattice, the number of involved patches $N_{LS}+N_{HS}=64\times64$ warrants reasonable statistics.

Figure 6(a) shows plots of S versus Y_A obtained simulating the ZGB model with local reconstruction. It follows that $S\rightarrow1$ for both $Y_A\rightarrow0$ and $Y_A\rightarrow Y_{Ac}\cong0.5035$. Furthermore, $S\rightarrow0$ for $Y_A=Y_{Am}\cong0.3310$. These results can be understood with the aid of Fig. 7 which shows the dependence of the average periods for the phases of low and high B_2 sticking coefficients; τ_{PL} and τ_{PH}, respectively, with Y_A. For $Y_A\rightarrow0$ one has that $\tau_{PL}\gg\tau_{PH}$ and consequently $N_{LS}\gg N_{HS}$ gives S-values close to unity; i.e., all patches are almost in the same surface state. Similarly, for $Y_A\rightarrow Y_{Ac}$ most
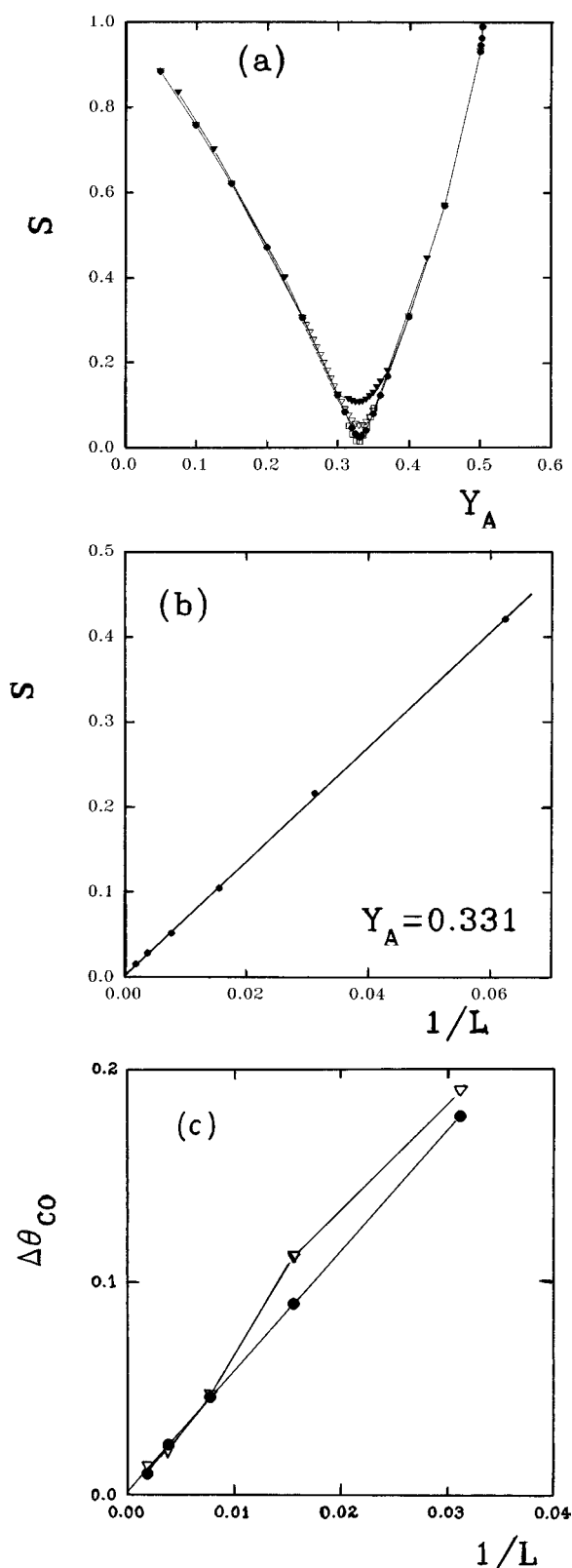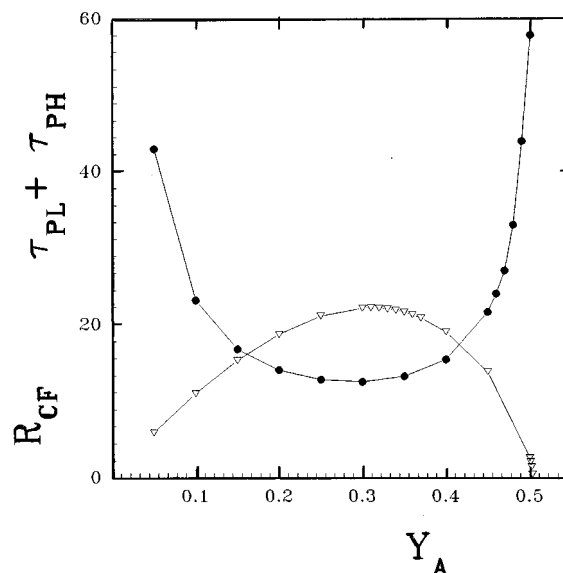
FIG. 7. ● Plot of $\tau_{PL} + \tau_{PH}$ vs Y_A for the ZGB model with global reconstructions. ▽ Plot of the normalized rate of reversible surface transformations R_{CF} vs Y_A for the ZGB model with local reconstructions ($L_p = 8$). The used lattice side is $L = 512$.

patches are in the phase with high B_2 sticking coefficient ($N_{LS} \ll N_{HS}$) due to the fact that A-coverage is close to poisoning, so one has $S \rightarrow 1$ again. Between these extreme regimes, just at Y_{Am}, one has $\tau_{PL} = \tau_{PH}$ which correspond to the minimum in the plot of $\tau_{PL} + \tau_{PH}$ versus Y_A (Fig. 7). Also, at this point the normalized rate of reversible surface transformations R_{CF} is maximum (Fig. 7) and $S \rightarrow 0$ (Fig. 6). Furthermore, just at Y_{Am} the patches of the surface may be in the two available surface states with the same probability and the following relationship may hold for the average number of patches:

$$\langle N_{LS} \rangle = \langle N_{HS} \rangle, \tag{5}$$

consequently the surface state order parameter is close to zero. (Notice that $S = 0$ only if $N_{LS} = N_{HS}$, as it will be discussed below). The state of the reactants on the surface at this particular point is shown in the snapshot configuration of Fig. 8. Here one can observe almost the same population of clusters of A- and B-species, as discussed above. Clusters of different species are surrounded by empty sites and precisely at these sites the reaction occurs upon adsorption of reactants from the gas phase. This means that the rate limiting step of the reaction is due to the available vacant sites at the perimeter of the clusters, since the bulk of such clusters are catalytically inactive. Furthermore, the snapshot of Fig. 8 shows the absence of large clusters of the same type of patch.

Let us now discuss the finite size effects on S which can be observed in Fig. 6(a) at Y_{Am}. In finite samples one has $\tau_{PL} = \tau_{PH}$ and Eq. (5) holds for the average number of patches. Due to the fluctuations which occur in the finite system one has $N_{LS} \neq N_{HS}$ for most time instants. So, the order parameter is close to zero but does not vanish exactly. Pointing now our attention to the thermodynamic limit, one has that $\tau_{PL} = \tau_{PH}$ still holds because it is a characteristic of the individual patches. However, in the $L \rightarrow \infty$ limit the total
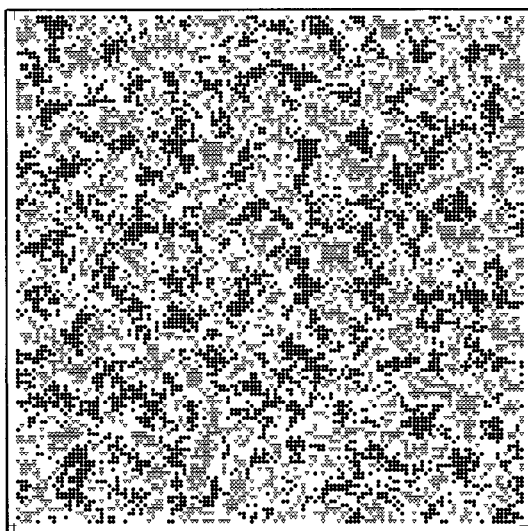
FIG. 6. Plots of the surface structure order parameter S the ZGB model with local reconstructions and $L_p = 8$. (a) Plots of S vs Y_A for lattices of different side: ▼ $L = 64$, ▽ $L = 128$, ● $L = 256$, and □ $L = 512$. (b) Plot of S vs $1/L$ obtained for $Y_A = Y_{Am} = 0.3310$. Note that $S(L \rightarrow \infty) \rightarrow 0$. (c) Plots of the amplitude of the oscillations in the coverage with A-species ($\Delta \theta_{CO}$) vs $1/L$ obtained for (●) $Y_A = 0.10$ and (▽) $Y_A = 0.20$, respectively. Note that $\Delta \theta_{CO}(L \rightarrow \infty) \rightarrow 0$.

FIG. 8. Snapshot configuration of the catalyst surface obtained at $Y_A = 0.3310 \cong Y_{Am}$. $\triangledown$ B-species, $\bullet$ A-species. Empty sites are left white. Notice the formation of clusters of both species surrounded by empty sites.

number of patches also diverges and, more interesting, Eq. (5) holds exactly (not only in the average), that is $N_{LS} = N_{HS} \rightarrow \infty$. So, under this condition one may expects $S(L \rightarrow \infty) = 0$ as it is shown in Fig. 6(b).

An open key question is whether the system will display oscillations at all in the thermodynamic limit ($L \rightarrow \infty$) and for a very long measurement time. Of course, an unambiguous answer will require a finite-size scaling analysis using larger lattices than those of the present work ($L = 512, L_p = 8$). Regrettably, this task is beyond our computational capabilities. The fact that $S(L \rightarrow \infty) = 0$ at Y_{Am} strongly suggest that the oscillations of the system will vanish in the thermodynamic limit due to compensatory effects. Concerning the reactive regime with $Y_A \neq Y_{Am}$ one has that in the thermodynamic limit $\tau_{PL} \neq \tau_{PH}$ and $N_{LS} \neq N_{HS}$. So, compensatory effects are not longer expected, consequently $S(L \rightarrow \infty) \neq 0$ and additional studies are requested. The dependence of the amplitude of the oscillations ($\Delta \theta_{CO}$) on the system size has been measured as it is shown in Fig. 6(c). This evidence indicates that for the whole reactive regime and local reconstructions, oscillations are restricted to finite samples.

An essential feature for the observation of oscillations at global scale in the thermodynamic limit is the occurrence of correlations among all patches. So, there should be at least one mechanism operating at local scale, capable to spread out the information throughout the sample. In principle one may identify two of such mechanisms: dimer adsorption and reaction events at neighboring patches. Nevertheless, since our finite size analysis shows that oscillations vanish in the thermodynamic limit, the correlations constructed by the operation of such mechanisms do not diverge at all and are restricted to short distances.

IV. CONCLUSIONS

The well known ZGB model for a dimer–monomer lattice-gas reaction process of the type $A + (\frac{1}{2})B_2 \rightarrow AB$ is

generalized in order to account for adsorbate-induced reversible transitions in the structure of the catalyst. Results of the proposed model assuming global reconstructions of the surface are in qualitative agreement with at least two relevant experimental facts, which are well documented for the catalytic oxidation of carbon monoxide on platinum surfaces: (i) The coverage with the reactants and the rate of production exhibit oscillatory behavior, and (ii) a sharp transition between the reactive regime and the A-poisoned state is observed.

The observed oscillatory behavior is due to the coupling between the surface structure and the sticking coefficient of B_2-species. Considering global reconstructions of the surface driven by the average surface coverage well defined periodic and nonperiodic oscillations are observed. However, considering the local reconstruction of small patches of the surface, also driven by local coverages, the oscillations become more irregular and a study of finite size effects shows that they are restricted to finite samples (oscillations vanish in the thermodynamic limit).

The proposed model is, so far, an improved version of the original ZGB-model, pointing out that the introduced surface reconstruction, coupled to the coverage with the reactants, is essential for a more realistic study of the reaction of the oxidation of carbon monoxide on some catalysts. Within this context it is worth studying the influence of A-diffusion and desorption on the predictions of the new model, a matter which is under progress. In fact, recently Vigil et al.[23] have reported that the onset of self-sustained oscillations, in a variant of the ZGB model, take place when the ratio between the hopping constant and the reaction rate constant exceeds some threshold close to ten.

[1] E. V. Albano, Heterog. Chem. Rev. **3**, 389 (1996).
[2] R. M. Ziff, E. Gulari, and Y. Barshad, Phys. Rev. Lett. **56**, 2553 (1986).
[3] J. W. Evans, Langmuir **7**, 2514 (1991).
[4] V. P. Z. Zhdanov and B. Kasemo, Surf. Sci. Rep. **20(3)**, 111 (1994).
[5] M. Ehsasi et al., J. Chem. Phys. **91**, 4949 (1989).
[6] K. Christmann, in Introduction to Surface Physical Chemistry, edited by H. Baumgartel, E. U. Franck, and W. Grunbein (Springer-Verlag, New York, 1991).
[7] J. W. Evans and M. S. Miesch, Surf. Sci. **245**, 401 (1991).
[8] J. W. Evans and M. S. Miesch, Phys. Rev. Lett. **66**, 833 (1991).
[9] R. M. Ziff and B. J. Brosilow, Phys. Rev. A **46**, 4630 (1992).
[10] B. J. Brosilow and R. M. Ziff, Phys. Rev. A **46**, 4534 (1992).
[11] E. V. Albano, Appl. Phys. A: Solids Surf. **55**, 226 (1992).
[12] G. Grinstein, Z.-W. Lai, and D. A. Browne, Phys. Rev. A **40**, 4820 (1989).
[13] I. Jensen, H. Fogedby, and R. Dickman, Phys. Rev. A **41**, 3411 (1990).
[14] E. V. Albano, Phys. Rev. E **49**, 1738 (1994).
[15] P. Meakin and D. J. Scalapino, J. Chem. Phys. **87**, 731 (1987).
[16] P. Grassberger and A. De La Torre, Ann. Phys. (N.Y.) **122**, 373 (1979); and P. Grassberger, J. Phys. A **22**, 3673 (1989).
[17] H. P. Kaukonen and R. M. Nieminen, J. Chem. Phys. **91**, 4380 (1989).

[18] J. J. Luque, F. Jiménez-Morales, and M. C. Lemos, J. Chem. Phys. **96**, 8535 (1992).

[19] J. Satulovsky and E. V. Albano, J. Chem. Phys. **97**, 9440 (1992).

[20] R. Imbihl, Prog. Surf. Sci. **44**, 185 (1993).

[21] R. Imbihl and G. Ertl, Chem. Rev. **95**, 697 (1995).

[22] P. Moller, K. Wetzl, M. Eiswirth, and G. Ertl, J. Chem. Phys. **85**, 5328 (1986).

[23] R. D. Vigil and F. T. Wilmore, Phys. Rev. E **54**, 1225 (1996).

[24] A. López and E. V. Albano (to be published).